ELSEVIER

Ceramics International 33 (2007) 773–778

CERAMICS
INTERNATIONAL

www.elsevier.com/locate/ceramint

Effect of B_2O_3 on crystallization behavior and microstructure of $MgO–SiO_2–Al_2O_3–K_2O–F$ glass–ceramics

A. Faeghi-Nia [a], V.K. Marghussian [b], E. Taheri-Nassaj [a,*]

[a] *Department of Materials Science and Engineering, Tarbiat Modares University, P.O. Box 14155-143, Tehran, Iran*
[b] *Ceramic division, Department of Materials, Iran University of Science and Technology, Narmak, Tehran 16844, Iran*

Received 9 December 2005; received in revised form 23 December 2005; accepted 30 January 2006

Abstract

The crystallization behavior of fluorphlogopite, a glass–ceramic located in $MgO–SiO_2–Al_2O_3–K_2O–F$ system was studied by varying the B_2O_3 content in the glass composition. DTA, XRD and scanning electron microscopy (SEM) were used for the study of crystallization behavior and microstructure of resulting glass–ceramics.

Heat treatment of glass specimens in the form of pressed powders in 600–950 °C range led to the formation of MgF_2 and fluorphologopite. DTA analysis revealed that the first peak crystallization temperatures (T_{c1}) and glass transition temperature (T_g) decreased by increasing B_2O_3 content, while the crystallization temperature increased with increasing the particle size of each composition.

DTA and XRD results indicated that the phlogopite crystallites probably transform from monoclinic to trigonal (3t) polytype at a temperature in the range of 950–1000 °C.

It was also shown that the higher the B_2O_3 content, the higher the aspect ratio of the phlogopite crystals.

Keywords: Glass–ceramic; Fluorphlogopite; B_2O_3; Crystallization

1. Introduction

Fluormica glass–ceramics are the basis of machinable ceramics that can be cut, drilled and turned with conventional tools [1–3]. Most of the commercial machinable glass–ceramics are based on potassium fluorphlogopite. Despite the widespread commercial use of the above-mentioned materials, relatively few systematic studies have been published concerning the effect of composition on crystallization behavior and microstructure of fluorophlogopite glass–ceramics in general.

Hoda and Beall [4] investigated barium, calcium and strontium containing phlogopites, Uno et al. [5] investigated barium fluorphlogopites with higher mechanical strength and toughness in comparison with potassium containing fluorphlogopites. Henry and Hill [6] studied the influence of alumina content on the crystallization behavior of barium fluorphlogopites and the influence of lithia on the nucleation and crystallization behavior of barium fluorphlogopites [7].

In this respect the addition of B_2O_3 to these glass compositions has still attracted less attention. Beall [8] mentioned that the aspect ratio of fluorophlogopite crystals increases by B_2O_3 addition.

In this work the effect of B_2O_3 addition on crystallization details of potassium fluorphlogopite glass–ceramics has been investigated.

2. Experimental procedure

The mixtures of reagent grade chemicals, K_2CO_3, $MgCO_3$, H_3BO_3, Al_2O_3 and pure optical grade silica, were melted in zircon crucibles at temperatures ranging from 1400 to 1440 °C in an electric furnace for 1–2 h. The resulting melts were quenched in cold distilled water. All glass frits were completely amorphous by XRD. The chemical composition of glasses is displayed in Table 1. It can be seen that SiO_2 was replaced by B_2O_3 in 3 wt% steps in base glass composition (B).

The frits were ground in an agate mortar, ball milled and sieved to give fine (<45 μm) and coarse (1–2 mm) particles for subsequent use in DTA analysis. DTA analysis, which was

---

* Corresponding author. Tel.: +98 21 88011001; fax: +98 21 88006544.
E-mail address: taheri@modares.ac.ir (E. Taheri-Nassaj).

0272-8842/$32.00 © 2006 Elsevier Ltd and Techna Group S.r.l. All rights reserved.
doi:10.1016/j.ceramint.2006.01.022

Table 1
Compositions of studied glass

Wt%	SiO_2 (wt%)	MgO (wt%)	K_2O (wt%)	B_2O_3 (wt%)	Al_2O_3 (wt%)	F (wt%)
B	46	22	9	3	14	6
M1	43	22	9	6	14	6
M2	40	22	9	9	14	6
M3	37	22	9	12	14	6
M4	34	22	9	15	14	6

utilized to determine the crystallization temperature of glasses, was performed by using 6 mg of glass powders in an alumina crucible in air with a heating rate of 20 °C min^{-1}.

The glass powders were mixed with 2.5 wt% polyvinyl alcohol as a binder and pressed into 59 mm × 13 mm × 5 mm bars at a pressure of 100 MPa using a laboratory uniaxial hydraulic press. The heat treatment was performed at 650, 800, 900, 950 and 1050 °C for 1 h with a heating rate of 20 °C min^{-1} in an electric furnace. The crystallization products were identified by XRD and the microstructures were inspected using scanning electron microscopy (SEM).

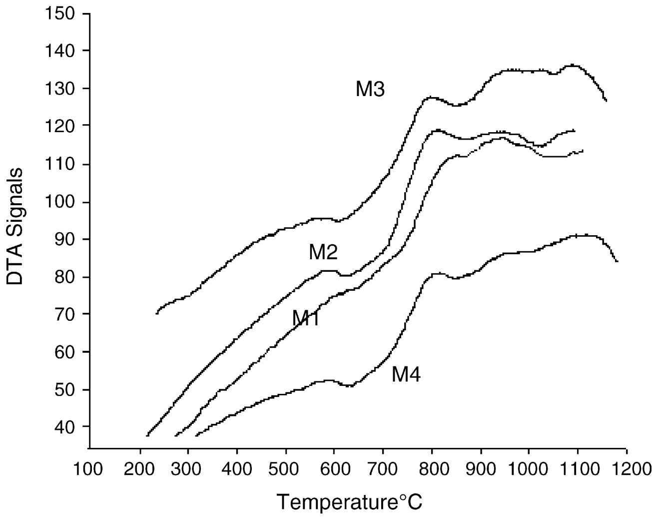

Fig. 1. DTA traces for fine particle size specimens (<45 μm).

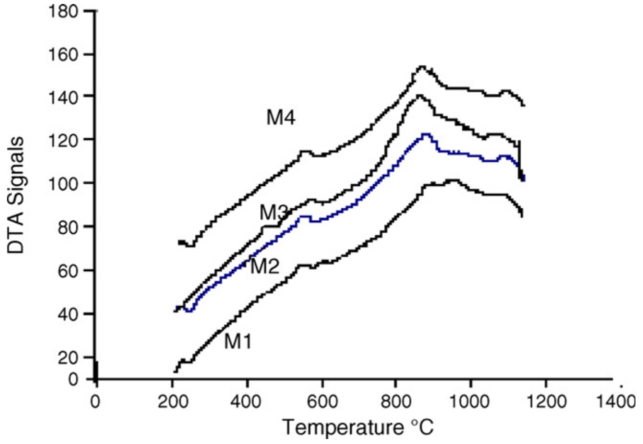

Fig. 2. DTA traces for coarse particle size specimens (1 mm).

3. Results and discussion

Figs. 1 and 2 represent DTA traces for the fine and coarse particle size glasses, respectively.

A relatively large shift in the first exothermic DTA peak of the coarse particle size specimen relative to the fine particle size

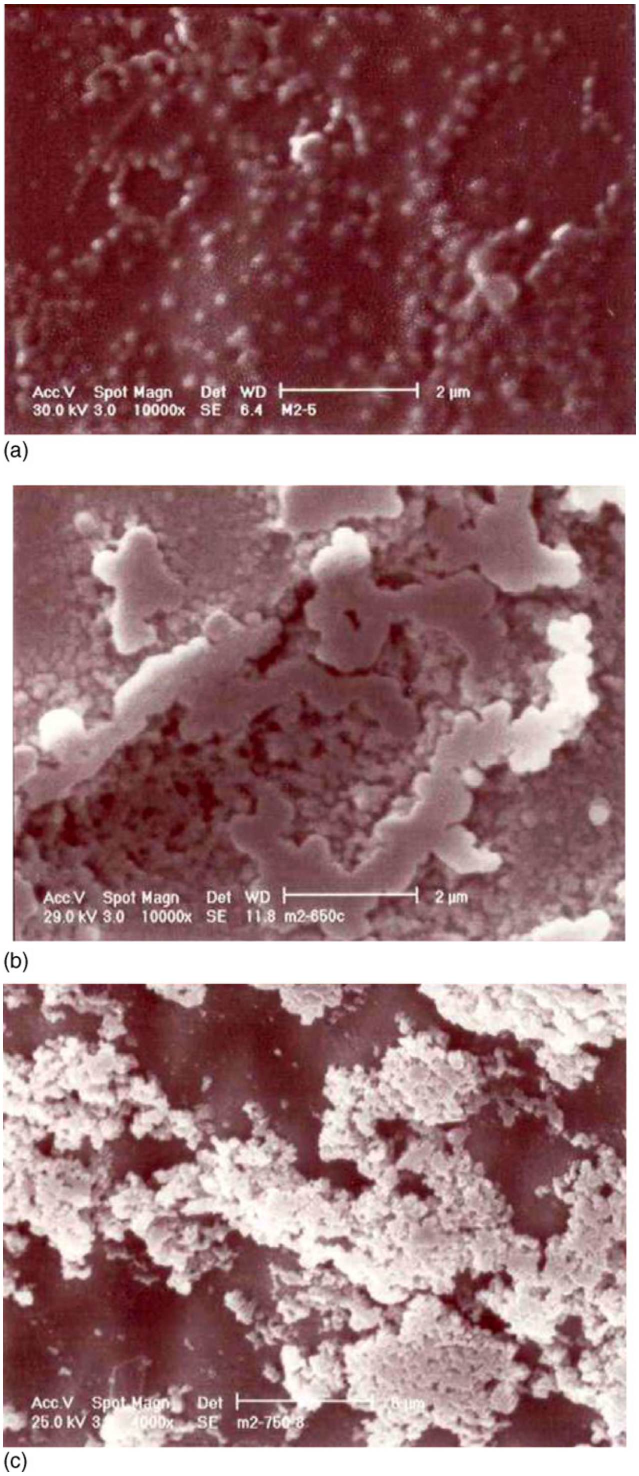

Fig. 3. Glass specimen M1: (a) as quenched, showing phase separation; (b) heat treated at 650 °C showing dendritic growth; and (c) heat treated at 800 °C showing crystalline clusters of MgF_2.

Table 2
List of glass transition temperatures, softening points, crystallization temperatures

Glass sample	Grain size	T_g (°C)	T_d (°C)	T_{c1} (°C)
M1	<45 μm	602	639	822
M2	<45 μm	590	623	819
M3	<45 μm	587	612	817
M4	<45 μm	560	608	798
M1	1 mm	600	630	909
M2	1 mm	590	630	889
M3	1 mm	580	630	880
M4	1 mm	550	580	878

($\Delta T = 60$–80 °C) can be taken as an indication of a marked tendency towards surface crystallization. Table 2 summarizes the DTA results.

It can be deduced from Figs. 1 and 2 and Table 2 that exo-peak temperatures as determined by DTA, are a function of B_2O_3 content and gradually decrease as B_2O_3 increases.

A significant decrease in viscosity occurring due to the addition of B_2O_3, which is apparent from the considerable drop in glass transition temperature (T_g) and dilatometric softening point (T_d) temperatures of glass specimens (Table 2), resulted in higher mobilities for different ions and ionic complexes operative in crystallization process of glasses. This leads to elevated crystallization rates and lower exo-peak temperatures.

4. Microstructural investigations

Figs. 3 and 4 reveal the sequence of crystallization processes in some specimens.

It is clear that as quenched glasses M1 and M3 exhibit a liquid–liquid phase separation (Figs. 3a and 4a). The droplet phases were found to be MgO-rich glasses, while matrix glasses were rich in SiO_2, according to EDX analysis (Fig. 5).

It seems that the liquid droplets in specimen M3, which are about 2 μm in mean diameter, are much larger than droplets in specimen M1. This can be attributed to lower viscosity values and higher ionic mobilities leading to faster growth rates in these specimens.

By heating the specimens to a temperature higher than 600 °C, they undergo a complex crystallization process that eventually leads to the formation of fluorphlogopite crystals. Figs. 3 and 4b depict SEM micrographs of the above specimens showing the dendritic growth of some apparently crystalline particles over the phase-separated areas, at 650 °C.

It has been reported [6] that chondrodite first nucleates preferentially along the liquid droplet surfaces and then undergoes a dendritic growth into the MgO-rich matrix in the glasses of this system. The residual glass was believed to have a boro-alumino-silicate composition that may be phase separated. Neither chondrodite nor any other crystalline phase was detected by XRD after heat treatment at 650 °C in the present work. It is possible that the low content of the crystalline phases prevented their detection.

Results shown in Fig. 6 reveals that by heating the specimen M1 to 800 °C, MgF_2 crystals have formed as the sole crystalline phase, but in the case of specimen M3 phlogopite has accompanied the MgF_2 phase.

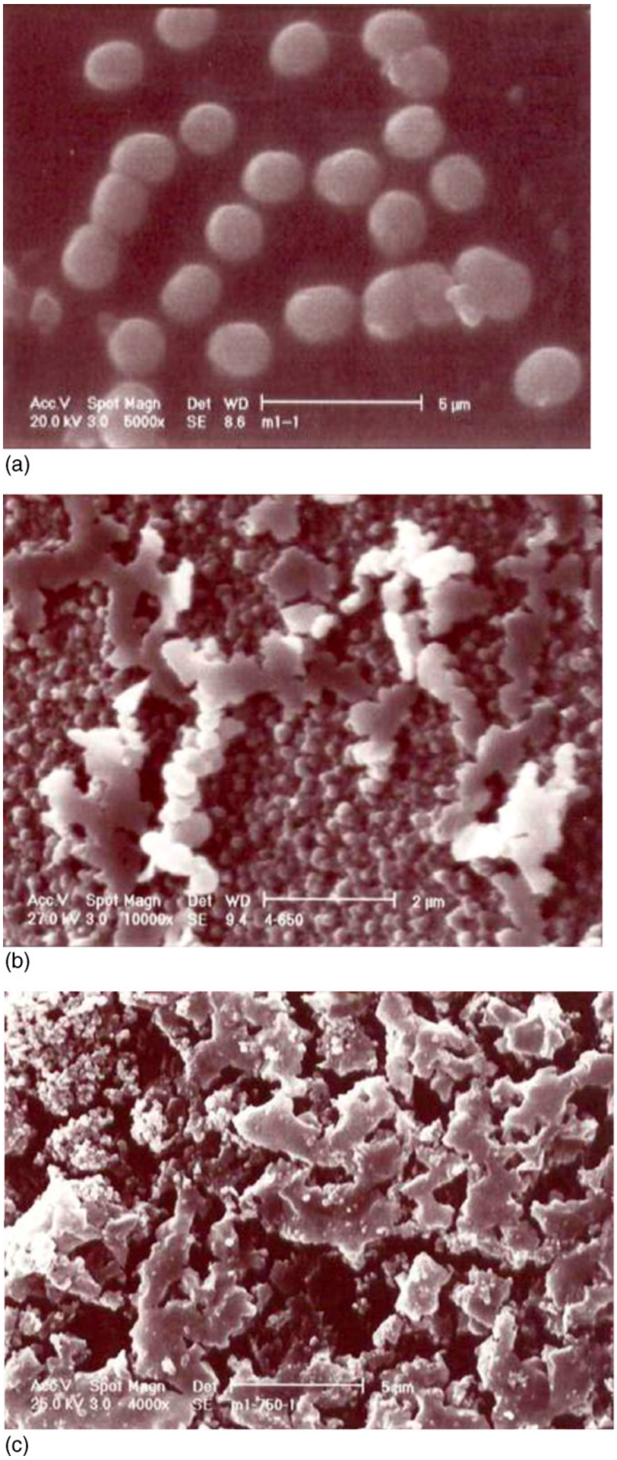

(a)

(b)

(c)

Fig. 4. Glass specimen M3: (a) as quenched, showing phase separation; (b) heat treated at 650 °C showing dendritic growth; and (c) heat treated at 800 °C showing clusters of MgF_2 crystals alongside plate-like particles of phlogopite.

Fig. 3c depicts the clusters of MgF_2 crystals in specimen M1 and Fig. 4c shows the plate-like crystals of phlogopite alongside the clusters of MgF_2 crystals in specimen M3.

It was reported that [9] a solid state reaction between the chondrodite and liquid droplets results in MgF_2 formation and,

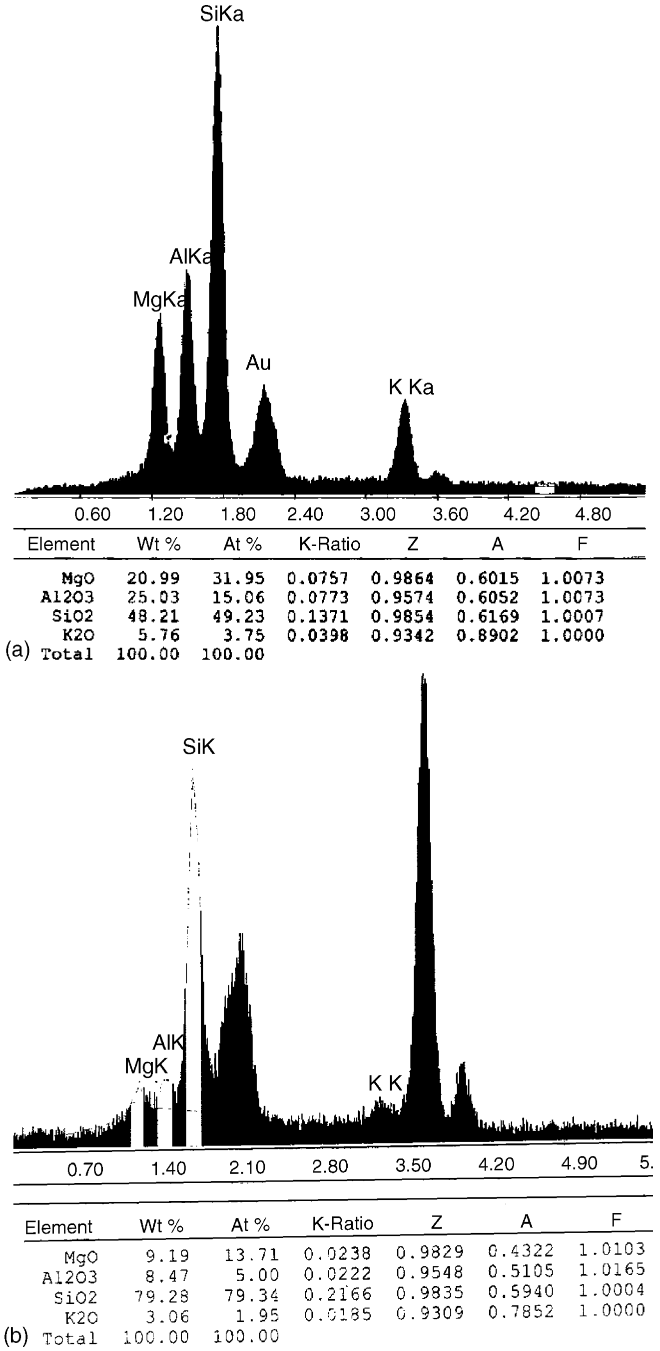

(a)

Element	Wt %	At %	K-Ratio	Z	A	F
MgO	20.99	31.95	0.0757	0.9864	0.6015	1.0073
Al2O3	25.03	15.06	0.0773	0.9574	0.6052	1.0073
SiO2	48.21	49.23	0.1371	0.9854	0.6169	1.0007
K2O	5.76	3.75	0.0398	0.9342	0.8902	1.0000
Total	100.00	100.00				

(b)

Element	Wt %	At %	K-Ratio	Z	A	F
MgO	9.19	13.71	0.0238	0.9829	0.4322	1.0103
Al2O3	8.47	5.00	0.0222	0.9548	0.5105	1.0165
SiO2	79.28	79.34	0.2166	0.9835	0.5940	1.0004
K2O	3.06	1.95	0.0185	0.9309	0.7852	1.0000
Total	100.00	100.00				

Fig. 5. EDX analysis of as received glass M3 (a) droplet phases (b) matrix phase.

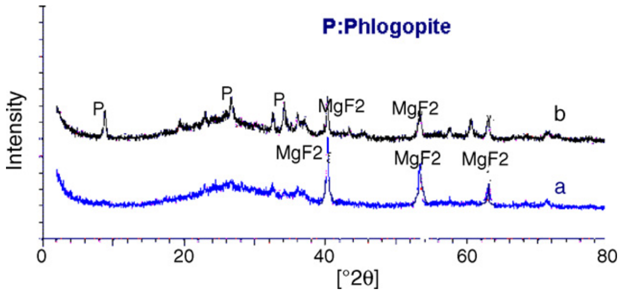

Fig. 6. XRD patterns of (a) specimen M1 and (b) specimen M3 after heat treatment at 800 °C for 1 h.

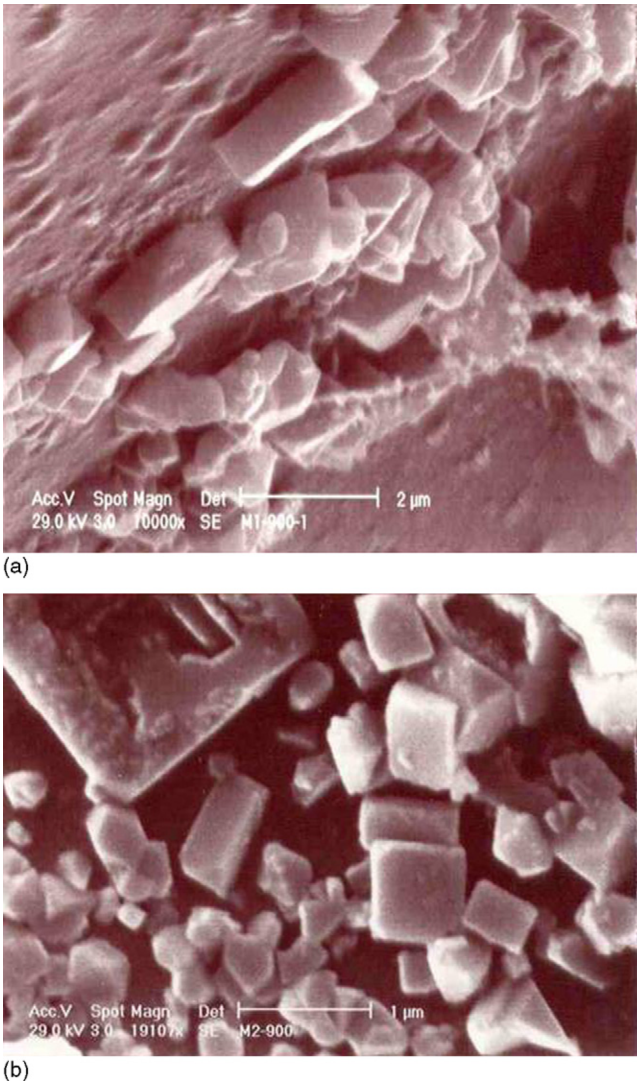

Fig. 7. SEM micrographs of (a) specimen M1 and (b) specimen M3 heat treated at 900 °C for 1 h.

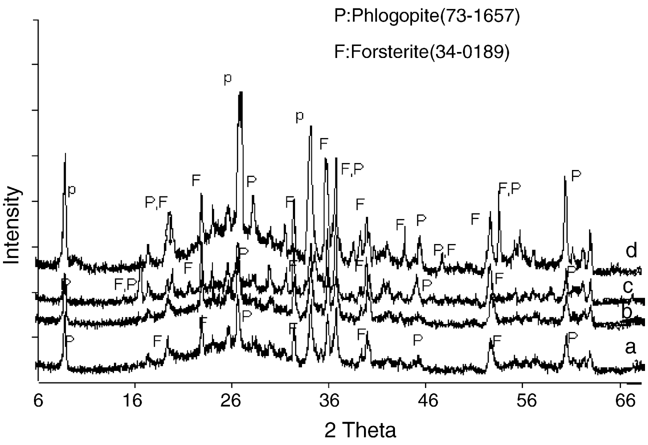

Fig. 8. XRD patterns of specimens (a) M1, (b) M2, (c) M3 and (d) M4 heat treated at 900 °C for 1 h.

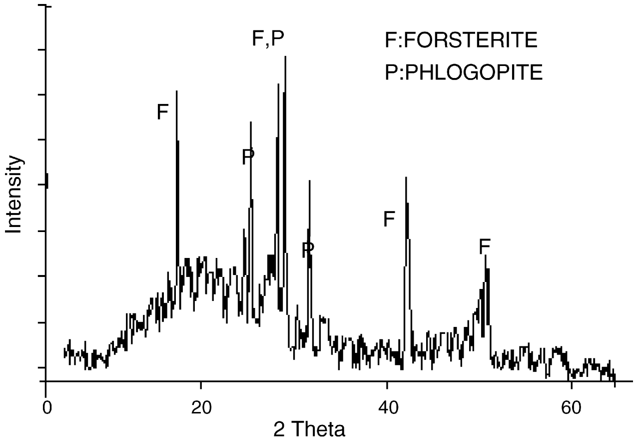

Fig. 9. XRD patterns of specimen M3 heat treated at 950 °C. The principal peak of phlogopite at $2\theta = 8°$ has disappeared.

on the other hand, from a crystal chemical point of view the epitaxial growth of mica on MgF_2 crystals is possible.

In the case of specimen M3, the formation of two phases can be attributed to the lower viscosity of the glass resulting in higher reaction rates involving MgF_2 crystals and the glassy phase, leading to the formation of phlogopite crystals.

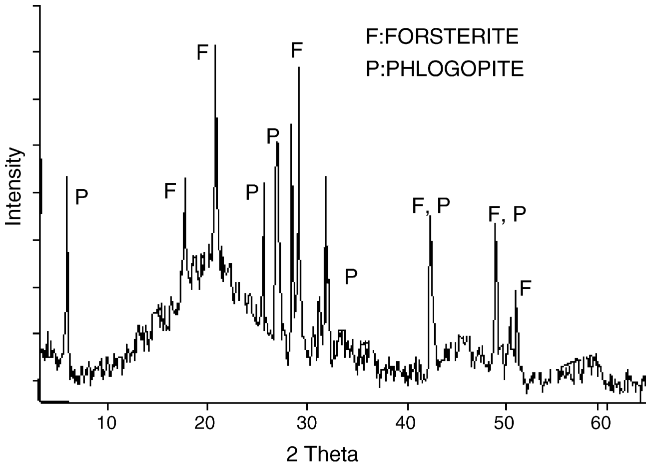

Fig. 10. XRD pattern of specimen M3 heat treated at 1050 °C showing the reappearance of the principal peak of phlogopite at $2\theta = 8°$.

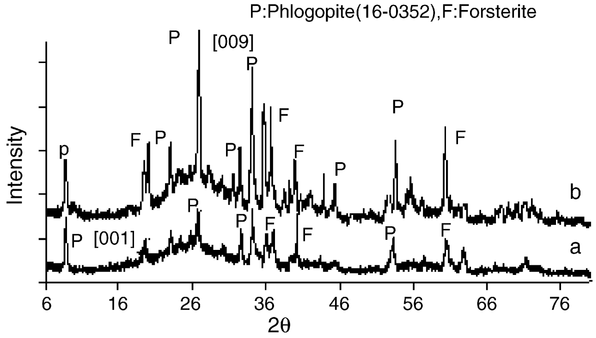

Fig. 11. XRD patterns of specimen M3 (a) heat treated at 840 °C, the reflection of [0 0 1] planes is dominant and (b) heat treated at 1050 °C, the reflection of [0 0 9] planes is dominant.

In Fig. 7a and b, the blocky morphology of phlogopite crystals can be observed in specimens M1 and M3 heat treated at 900 °C. XRD patterns shown in Fig. 8 indicate the existence of forsterite and phlogopite phases.

It was suggested that the loss of silicon tetrafluoride from the surface of glass specimens, by reducing the fluorine content,

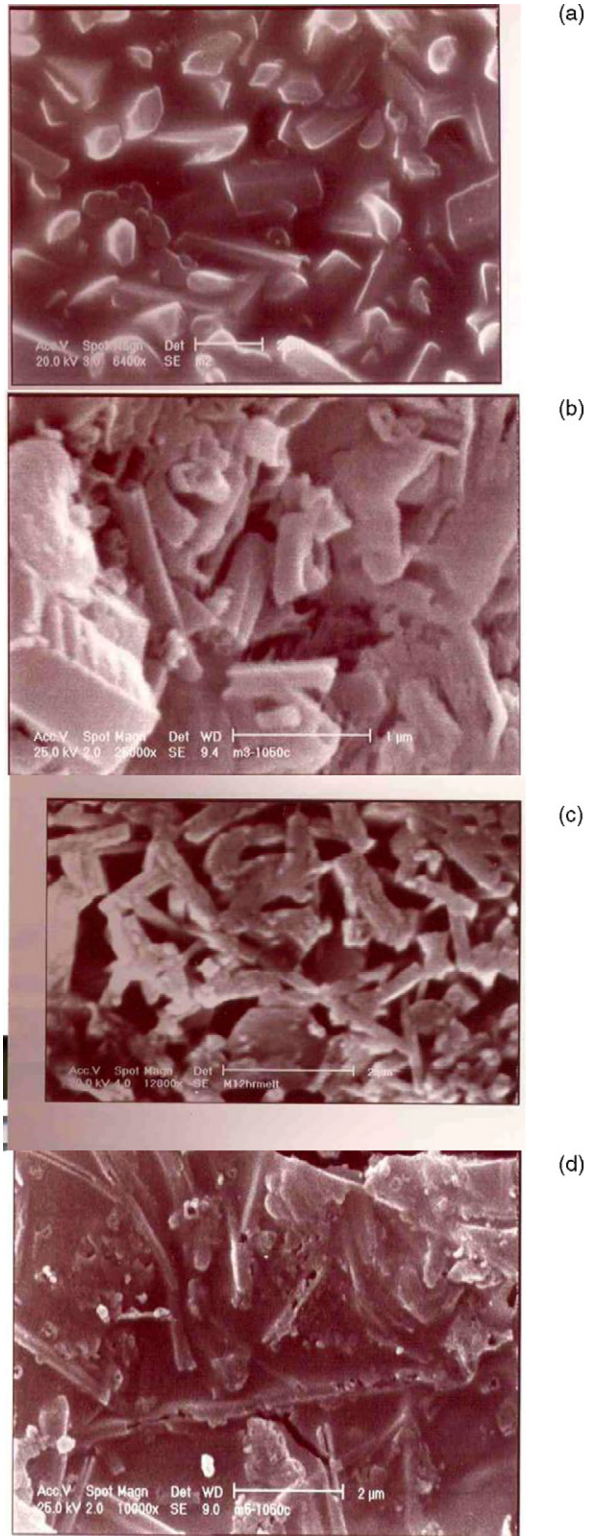

Fig. 12. SEM micrographs of specimens (a) M1 (b) M2 (c) M3 and (d) M4 heat treated at 1050 °C for 1 h.

leaves a residual glass rich in silicon and magnesium [6]. It can be proposed that this glass phase subsequently may crystallize to forsterite.

The presence of a second exo-peak in the DTA curves, around 900 °C probably indicates the forsterite formation.

After the heat treatment of specimens at 950 °C, the intensity of the principal diffraction lines of phlogopite especially at $2\theta = 8^\circ$ decline.

This especially occurred in sample M3 containing higher amounts of B_2O_3 in which the diffraction line corresponding to $2\theta = 8^\circ$ has been completely disappeared. Fig. 9 shows XRD results for this specimen.

According to DTA traces there are weak endothermic effects observable at $T > 950$ °C which probably can be related to a disordering process involving the structure of phlogopite crystals.

By increasing the heat treatment temperature to 1050 °C the principal XRD peak of phlogopite at $2\theta = 8^\circ$ reappears (Fig. 10). On the other hand, Fig. 11 indicates that in specimens heat treated at lower temperatures, diffraction lines relating to [0 0 1] planes are predominant which may be associated with monoclinic system whereas in higher temperatures, the diffraction lines of [0 0 9] planes are predominant which can be related to trigonal system.

This finding probably indicates the occurrence of a transformation from monoclinic to trigonal structure for phlogopite crystals at high temperatures in the range of 950–1050 °C.

The resultant micrographs of the specimens heat treated at 1050 °C (Fig. 12) displays a marked difference in crystal aspect ratios.

The phlogopite crystals in samples M3 and M4 exhibit aspect ratios of about 10 and 15, respectively, whereas the specimens M1 and M2 show lower aspect ratios of 2 and 5, respectively.

It can be proposed that replacement of SiO_2 by B_2O_3 via lowering the viscosity of glass samples and increasing the diffusion rates of ionic species [10], opens the way for crystals to display their natural tendency towards directional growth of rod shape crystals which otherwise might have been suppressed and controlled by slow diffusion rates.

5. Conclusions

The crystallization behavior of a glass–ceramic based on $KMg_3AlSi_3O_{10}F_2$ micas was studied by varying the B_2O_3 content in glass composition. Increasing the B_2O_3 content reduces the glass transition temperature, dilatometric softening point and first peak crystallization temperature (T_{c1}).

DTA results revealed the existence of a marked tendency towards surface crystallization in all glass specimens.

The specimens showed a distinct phase separation process, forming droplet shape particles dispersed in a SiO_2 rich matrix. The crystallization process carried out around the first peak crystallization temperature, developed MgF_2 as the sole detectable crystalline phase in specimens containing low amounts of B_2O_3, whereas the specimen containing higher amounts of B_2O_3 in the 12–15% range in addition to MgF_2 developed fluorphlogopite crystals.

All specimens developed forsterite along with the phlogopite phase upon heating to $T > 900$ °C. At a higher temperature of 950 °C the phlogopite phase undergoes a phase transformation resulting in a distinct disorder and disappearance of the principal XRD diffraction line of phlogopite and then recrystallized at 1050 °C in the form of well grown particles of phlogopite exhibiting an apparently trigonal crystal structure. The above transformation is more distinct in specimens containing higher amounts of B_2O_3. The aspect ratio of phlogopite crystals increased with increasing the heat treatment temperature as well as the B_2O_3 content in the composition of glass specimens. The highest aspect ratio ($\approx$15) was developed in specimens containing 15 wt% B_2O_3 heat treated at 1050 °C.

References

[1] G.H. Beall, in: L.L. Henchand, S.W. Friemen (Eds.), Advances in Nucleation and Crystallization in Glasses, American Ceramic Society, Westerville, 1971, p. 251.
[2] C.K. Chyung, G.H. Beall, D.G. Grossman, in: G. Thomas, R.M. Fulrathand, R.M. Fisher (Eds.), Microstructure and Mechanical Properties of Mica Glass–Ceramics in Electron Microscopy and Structure of Materials, Berkely University of California Press, 1972 , p. 1167.
[3] C.K. Chyung, G.H. Beall, D.G. Grossman, Fluorphlogopite mica glass–ceramics, in: Proceedings of the International Glass Congress, No. 14, Kyoto, Japan, Ceramic Society of Japan, (1974), pp. 33–40.
[4] S.N. Hoda, G.H. Beall, Alkaline earth mica glass–ceramics, in: J.H. Simmons, D.R. Uhlmann, G.H. Beall (Eds.), Advances in Ceramics: Nucleation and Crystallization in Glasses, vol. 4, The American Ceramic Society, Inc., Columbus, Ohio, 1982, p. 287.
[5] T. Uno, T. Kasuga, K. Nakjima, J. Am. Ceram. Soc. 74 (1991) 3139.
[6] J. Henry, R.G. Hill, Influence of alumina content on the nucleation crystallization and microstructure of barium fluorphlogopite glass–ceramics based on $8SiO_2 \cdot YAl_2O_3 \cdot 4MgO \cdot 2MgF_2 \cdot BaO$, J. Mater. Sci. 39 (2004) 2499–2507.
[7] J. Henry, R.G. Hill, The influence of Lithia content on the properties of fluorphlogopite glass–ceramics. I. Nucleation and crystallization behaviour, J. Non-Cryst. Solids 319 (2003) 1–12.
[8] G.H. Beall, Mica glass–ceramics, US Patent No. 3 801 295 (2 April 1974).
[9] H. Dalal, F. Davis, Beta spodumene–mica glass–ceramic. 1. Phase evolution and microstructure, Ceram. Bull. 56 (11) (1977) 257–262.
[10] B. Aitken, G. Beall, Glass–ceramics, in: R.W. Cahn, P. Haasen, E.J. Kramer (Eds.), Ceramic Processing, Materials Science and Technology, vol. 11, VCH, Weinheim, New York, 1994, p. 291.